Wrapping Nanocrystals with an Amphiphilic Polymer Preloaded with Fixed Amounts of Fluorophore Generates FRET-Based Nanoprobes with a Controlled Donor/Acceptor Ratio

ARTICLE *in* LANGMUIR · APRIL 2009

Impact Factor: 4.46 · DOI: 10.1021/la8038347 · Source: PubMed

Wrapping Nanocrystals with an Amphiphilic Polymer Preloaded with Fixed Amounts of Fluorophore Generates FRET-Based Nanoprobes with a Controlled Donor/Acceptor Ratio

Aleksey V. Yakovlev,[†,‡,§,||,○] Feng Zhang,[⊥,○] Ali Zulqurnain,[⊥] Abbasi Azhar-Zahoor,[⊥] Camilla Luccardini,[†,‡,§,||] Stéphane Gaillard,[#] Jean-Maurice Mallet,[#] Patrick Tauc,[▽] Jean-Claude Brochon,[▽] Wolfgang J. Parak,*[,⊥] Anne Feltz,*[,||] and Martin Oheim*[,†,‡,§]

INSERM, U603, Paris F-75006, France, CNRS UMR 8154, Paris F-75006, France, Laboratory of Neurophysiology and New Microscopies, University Paris Descartes, 45 rue des Saints Pères, Paris F-75006, France, ENS-CNRS, UMR 8544, Laboratoire de Neurobiologie, Département de Biologie, Ecole Normale Supérieure, 46 rue d'Ulm, Paris F-75005, France, Department of Physics, Biophotonics, Philipps University of Marburg, Renthof 7, Marburg D-35037, Germany, ENS-CNRS, UMR 8642, Glycoscience, Département de Chimie, Ecole Normale Supérieure, 24 rue Lhomond, Paris F-75231, France, and ENS-CNRS, UMR 8113, Laboratoire de Biotechnologies et Pharmacologie génétique Appliquée (LBPA), Ecole Normale Supérieure de Cachan, 61 avenue du President Wilson, Cachan F-94235, France

Received November 19, 2008. Revised Manuscript Received December 22, 2008

Colloidal nanocrystal (NC) donors wrapped with a polymer coating including multiple organic acceptor molecules are promising scaffolds for fluorescence resonance energy transfer (FRET)-based nanobiosensors. Over other self-assembling donor−acceptor configurations, our preloaded polymers have the virtue of producing compact assemblies with a fixed donor/acceptor distance. This property, together with the possibility of stoichiometric polymer loading, allowed us to directly address how the FRET efficiency depended on the donor/acceptor. At the population level, nanoprobes based on commercial as well as custom CdSe/ZnS donors displayed the expected dose-dependent rise in transfer efficiency, saturating from about five ATTO dyes/NC. However, for a given acceptor concentration, both the intensity and lifetime of single-pair FRET data revealed a large dispersion of transfer efficiencies, highlighting an important heterogeneity among nominally identical FRET-based nanoprobes. Rigorous quality check during synthesis and shell assembly as well as postsynthesis sorting and purification are required to make hybrid semiconductor−organic nanoprobes a robust and viable alternative to organic or genetically encoded nanobiosensors.

Introduction

With their large absorbance permitting blue-shifted excitation remote from acceptor direct excitation, size-dependent tunable narrow emission, longer excited-state lifetime, and better photostability compared to organic chromophores, semiconductor nanocrystals (NCs) are potent donors for building fluorescence resonance energy transfer (FRET)-based nanoprobes.[1−7] Such nanosensors have been successfully used to detect toxins,[8] probe enzymatic activity,[9] screen for enzyme inhibitors,[10] or measure ion concentration.[11−13] In addition to offering new possibilities for ultrasensitive analyte detection, functionalized NCs provide an ideal platform for the attachment of multiple fluorophores, thereby increasing the FRET efficiency[2,4,12,14−17] or permitting the design of polyvalent sensors through acceptor multiplexing.[8,13,17,18]

In the past, nanoprobe assembly has typically involved a compromise between sensor performance and colloidal stability (reviewed in refs 19 and 20). Compact donor/acceptor assemblies

* Corresponding authors. E-mail: anne.feltz@ens.fr (A.F.); martin.oheim@univ-paris5.fr (M.O.); wolfgang.parak@physik.uni-marburg.de (W.J.P.)
[†] INSERM, U603.
[‡] CNRS UMR 8154.
[§] University Paris Descartes.
[||] ENS-CNRS, UMR 8544, Laboratoire de Neurobiologie, Département de Biologie.
[⊥] Philipps University of Marburg.
[#] ENS-CNRS, UMR 8642, Glycoscience, Département de Chimie.
[▽] ENS-CNRS, UMR 8113, Laboratoire de Biotechnologies et Pharmacologie génétique Appliquée (LBPA).
[○] These authors contributed equally.

(1) Willard, D. M.; Carillo, L. L.; Jung, J.; Van Orden, A. *Nano Lett.* **2001**, *1*, 469–474.
(2) Tran, P. T.; Goldman, E. R.; Anderson, G. P.; Mauro, J. M.; Mattoussi, H. *Phys. Status Solidi B* **2002**, *229*, 427–432.
(3) Medintz, I. L.; Goldman, E. R.; Lassman, M. E.; Mauro, J. M. *Bioconjugate Chem.* **2003**, *14*(5), 909–918.
(4) Clapp, A. R.; Medintz, I. L.; Mauro, J. M.; Fisher, B. R.; Bawendi, M. G.; Mattoussi, H. *J. Am. Chem. Soc.* **2004**, *126*(1), 301–310.
(5) Alphandéry, E.; Walsh, L. M.; Rakovich, Y.; Bradley, A. L.; Donegan, J. F.; Gaponik, N. *Chem. Phys. Lett.* **2004**, *388*, 100–104.
(6) Fernandez-Arguelles, M. T.; Yakovlev, A.; Sperling, R. A.; Luccardini, C.; Gaillard, S.; Medel, A. S.; Mallet, J. M.; Brochon, J. C.; Feltz, A.; Oheim, M.; Parak, W. J. *Nano Lett.* **2007**, *7*(9), 2613–2617.
(7) Lu, H.; Schöps, O.; Waggon, U.; Niemeyer, C. M. *J. Am. Chem. Soc.* **2008**, *130*, 4815–4827.
(8) Goldman, E. R.; Clapp, A. R.; Anderson, G. P.; Uyeda, H. T.; Mauro, J. M.; Medintz, I. L.; Mattoussi, H. *Anal. Chem.* **2004**, *76*, 684–688.
(9) Xu, C.; Xing, B.; Rao, J. *Biochem. Biophys. Res. Commun.* **2006**, *344*, 931–935.
(10) Shi, F.; Rosenzweig, N.; Roszenzweig, Z. *Anal. Chem.* **2007**, *79*, 208–214.
(11) Snee, P. T.; Somers, R. C.; Nair, G.; Zimmer, J. P.; Bawendi, M. G.; Nocera, D. G. *J. Am. Chem. Soc.* **2006**, *128*(41), 13320–13321.
(12) Pons, T.; Medintz, I. L.; Wang, X.; English, D. S.; Mattoussi, H. *J. Am. Chem. Soc.* **2006**, *128*(47), 15324–15331.
(13) Suzuki, M.; Husimi, Y.; Komatsu, H.; Suzuki, K.; Douglas, K. T. *J. Am. Chem. Soc.* **2008**, *130*(17), 5720–5725.
(14) Patolsky, F.; Gill, R.; Weizmann, Y.; Mokari, T.; Banin, U.; Willner, I. *J. Am. Chem. Soc.* **2003**, *125*(46), 13918–13919.
(15) Kim, J. H.; Stephens, J. P.; Morikis, D.; Ozkan, M. *Sens. Lett.* **2004**, *2*, 85–90.
(16) Levy, M.; Cater, S. F.; Ellington, A. D. *ChemBioChem* **2005**, *6*, 2163–2166.
(17) Medintz, I. L.; Clapp, A. R.; Brunel, F. M.; Tiefenbrunn, T.; Uyeda, H. T.; Chang, E. L.; Deschamps, J. R.; Dawson, P. E.; Mattoussi, H. *Nat. Mater.* **2006**, *5*(7), 581–589.
(18) Clapp, A. R.; Medintz, I. L.; Uyeda, H. T.; Fisher, B. R.; Goldman, E. R.; Bawendi, M. G.; Mattoussi, H. *J. Am. Chem. Soc.* **2005**, *127*, 18212–18221.
(19) Medintz, I. L. *Trends Biotechnol.* **2006**, *24*(12), 539–542.

10.1021/la8038347 CCC: $40.75
Published on Web 01/27/2009

favor high FRET efficiencies, but additional coating layers increasing their effective size have to be introduced to preserve solubility and colloidal stability. Also, polyethylene glycol (PEG), which is widely used for this purpose,[21,22] introduces a microenvironment that may restrict the access of the analyte to the acceptor on the NC surface. Conversely, the *post hoc* attachment of the acceptor to the already coated and functionalized NC considerably increases donor/acceptor separation and impairs FRET efficiency.

A factor that has limited sensor performance is that acceptor binding and NC coating have been usually considered as two independent steps. By far, most sensor geometries have in common that FRET is modulated by reversibly or irreversibly displacing the acceptor from the NC donor.[10,17] More recently, a pH sensitive donor/acceptor FRET pair has been described where the acceptor is tethered on the NC surface and analyte binding/unbinding modulates the overlap integral between donor photoluminescence (PL) emission and acceptor excitation and thus modifies the FRET efficiency.[11,13] However, upon analyte binding, most fluorescent indicators change fluorescence through a modulation of their quantum efficiency rather than their absorbance. Thus, in hybrid FRET-based nanoprobes built from such probes, the amount of acceptor fluorescence varies with analyte concentration, but the transfer efficiency is actually constant.

To benefit from the large spectrum of available ion indicators and purpose-tailored fluorescent probes, we designed FRET sensors that incorporate the acceptor directly into an amphiphilic polymer coating. We have previously shown that these probes minimize the acceptor/donor distance, thus permit high transfer efficiencies, and outperform conventional sensors in which the acceptor is added *post hoc*, after synthesis of the amphiphilic coat by surface functionalization.[6]

In the present work, we preloaded the polymer shell with variable amounts of acceptor to study the impact of changing the acceptor/donor ratio (A/D) at a fixed donor/acceptor distance. Taking donor quenching, shortening of the donor lifetime, or an increase in the sensitized acceptor fluorescence as a readout, we demonstrate that the detected transfer efficiency increases with the number of dye molecules but starts to saturate for as little as five acceptor dyes per NC donor. While population measurements closely followed the expected result for a multiple-acceptor transfer mechanism, single-pair FRET (spFRET) recordings revealed a large heterogeneity among nanoprobes, with respect to both their donor quenching and sensitized acceptor fluorescence, and the excited-state lifetime. Our study provides important guidelines for designing FRET-based nanobiosensors and highlights the importance of single-molecule experiments to reveal inner-batch heterogeneity and select for the best FRET sensors.

Materials and Methods

Nanocrystal Synthesis. Four kinds of NCs were used in the current experiments and included Evident NCs (Evidots 560, Evident Technologies, Inc., ED-C11-Tol-0560), Invitrogen NCs (Qdot 565 ITK organic quantum dots, #Q21731MP), and two batches of homemade NCs: one was CdSe without the ZnS shell, and the other was CdSe/ZnS. For Table 1, we determined for each batch the absorption/emission spectra, permitting the direct comparison of the extinction coefficients. Therefore, we could estimate the core size for all four kinds of NCs using the same calibration curve, neglecting the ZnS shell thickness (values in ref 23 are reported for the inorganic core only). Concentrations were determined by absorption measurements, using Beer−Lambert's law.

Table 1. Specifications of the Four Kinds of Nanocrystals Used

	1st peak[a]	$\varepsilon^{(peak)}$	D_i	D_e	A_s
Evident NCs	531	82 325.8	2.7	5.1	177.2
Invitrogen NCs	543	99 040.0	2.9	5.3	186.6
homemade CdSe/ZnS	535	87 334.1	2.8	5.2	180.1
homemade CdSe	523	73 683.1	2.6	5.0	172.0

[a] 1st peak, first exciton absorption peak (nm), obtained by UV−vis spectrometry; $\varepsilon^{(peak)}$, extinction coefficient at its first exciton peak (cm^{-1} M^{-1}), extracted according to ref 23; D_i, diameter of inorganic core (nm), extracted according to ref 23; D_e, effective diameter $= D_i + 2 \times 1.2$ (thickness of TOPO shell) (nm); A_s, surface area of NC $= 4\pi(D_e/2)^2$ (nm^2).

Stoichiometric ATTO−Polymer Embedding. The polymer coating procedure has been described elsewhere.[6,24] Briefly, solutions of different ATTO−polymer ratio were mixed with NC-containing chloroform solution. For the three batches of Evident NCs and the Invitrogen Qdots used, a ratio of 100 polymer motifs per nm^2 of the NC surface was used in the coating process. For the homemade NC batches, we used 50 polymer motifs per nm^2. In contrast to previous protocols,[25] no cross-linker was used in this step. The ATTO−polymer-coated NCs were finally redissolved in borate buffer (sodium borate, 50 mM, pH 12.0).

Donor−Acceptor Ratios. We estimate that 25% of active maleic anhydride rings can react with other molecules containing amino groups. Using a derivate of ATTO with an amino group (abs/em = 597/615 nm, ATTO-TEC GmbH, Germany), the dye was first dissolved in anhydrous chloroform upon sonication, and its concentration was determined by absorption measurements, assuming an extinction coefficient at 597 nm in chloroform of 120 000 M^{-1} cm^{-1}. To obtain different ratios of ATTO dye embedded in polymer, ATTO solution was mixed with polymer solution as detailed in the text in % (mol/mol) of ATTO to maleic anhydride rings. The mixture was left overnight at room temperature and at least three-times concentrated to dryness and redissolved to enhance the reaction efficiency. Finally, the polymer concentration was determined either from the final solvent volume or from the calculated ATTO concentration determined by UV−vis spectrometry. The absorption spectrum of ATTO was not affected by the polymer (data not shown).

Purification. All solutions of the functionalized and assembled NCs were concentrated by ultrafiltering (100 kDa MW cutoff, Millipore) and filtered on 0.2 μm filters (Millipore). Gel electrophoresis on 2% agarose (UltraPure, Invitrogen #15510027) in 0.5× TBE buffer (44.5 mM Tris-borate and 1 mM EDTA, pH 8.3; Sigma-Aldrich, #T3913) was used for purification and run at 100 V for 80−100 min. The separated bands of empty micelles (faster band, red color) and particles (slow band, green or yellow colors) were cut by distinguishing the different colors under the UV lamp.[6] The samples were extracted from the cut bands sealed in dialysis membranes (50 kD, Spectrolabs, #132544) by elution and finally concentrated again by 100 kD ultrafiltration.

Overlap Integrals, Quantum Yields, and Calculated Förster Distances and FRET Efficiencies. We assembled FRET-based nanoprobes by wrapping a central NC donor with an amphiphilic polymer coat into which were included during synthesis ATTO molecules at a stoichiometry ratio (Figure 1A). The choice of these FRET pairs was guided by the requirements (i) to have bright enough NC donors to obtain detectable single-pair FRET (spFRET), (ii) to optimize the overlap between NC photoluminescent emission and ATTO absorption, and (iii) to maximize separation of the donor and acceptor emission spectra to permit dual-color FRET detection.

(20) Somers, R. C.; Bawendi, M. G.; Nocera, D. G. *Chem. Soc. Rev.* **2007**, *3*, 579–591.
(21) Ballou, B.; Lagerholm, B. C.; Ernst, L. A.; Bruchez, M. P.; Waggoner, A. S. *Bioconjugate Chem.* **2004**, *15*(1), 79–86.
(22) Yu, W. W. *J. Am. Chem. Soc.* **2007**, *129*(10), 2871–2879.
(23) Yu, W. W.; Qu, L.; Guo, W.; Peng, X. *Chem. Mater.* **2003**, *15*(14), 2854–2860.
(24) Lin, C. A.; Sperling, R. A.; Li, J. K.; Yang, T. Y.; Li, P. Y.; Zanella, M.; Chang, W. H.; Parak, W. J. *Small* **2008**, *4*(3), 334–341.
(25) Pellegrino, T.; Manna, L.; Kudera, S.; Liedl, T.; Koktysh, D.; Rogach, A. L.; Keller, S.; Rädler, J.; Natile, G.; Parak, W. J. *Nano Lett.* **2004**, *4*(4), 703–707.

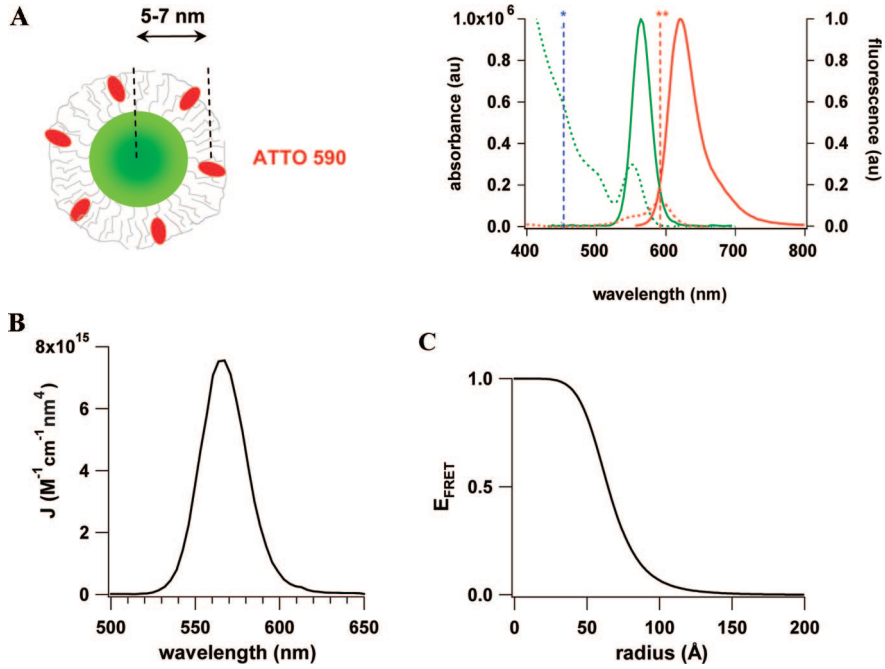

Figure 1. Overlap integrals, quantum yields, and calculated Förster distances and transfer efficiencies between Evident NC donors and ATTO590 dye: (A) Left: Cartoon showing the polymer-wrapped nanocrystal (NC)/ATTO dye assembly. Right: Absorbance (dotted) and normalized emission spectra (solid) of NC donor (green) and ATTO acceptor (red). Asterisk and double asterisk identify 450 and 590 nm wavelengths used for donor and direct (acceptor) excitation. (B) Calculated overlap integral and (C) FRET efficiency, assuming a r^6 dipole−dipole coupling. Förster radius R_F = 64.5 Å; $J = 7.75218 \times 10^{15}$ M^{-1} cm^{-1} nm^4.

We note that there is considerable uncertainty in the molar extinction ε of the NC donors, as different sources give different extinction coefficients (e.g., for Invitrogen NC at 543 nm, the manufacturer's data and measured data differ by a factor of 2; and similar discrepancies were observed by others[23,26] and might represent batch-to-batch variability). For consistency, all numbers reported were derived from the same calibration curve.[23,26]

We calculated the overlap integral

$$J = \int \mathrm{d}\lambda\, F_D(\lambda)\, \varepsilon_A(\lambda)\lambda^4 \tag{1}$$

which quantifies the normalized and dimensionless spectral overlap between donor emission $F_D(\lambda)$ and acceptor absorbance, $\varepsilon_A(\lambda)$, and R_0 the Förster radius, which is defined as the distance between the donor and acceptor that yields 50% energy-transfer efficiency (in $Å^6$),

$$R_0^{\,6} = 8.8 \times 10^{23} \kappa^2 n_D^{-4} Q_D J \tag{2}$$

Here, Q_D is the photoluminescence quantum yield of the NC donor in the absence of an acceptor, n_D is the refractive index of the medium (here, 1.33 for water at ~590 nm), and $\kappa^2 = 2/3$ is the orientation factor, assuming random orientation between the NC and ATTO dipoles.

We derived the transfer efficiency from the quenching of donor photoluminescence, or decrease in donor lifetime in the presence of the acceptor, according to

$$E^{(a)} = 1 - F_{DA}/F_D \tag{3a}$$

or from the sensitized acceptor fluorescence,

$$E^{(b)} = \frac{\varepsilon_A(\lambda_D)}{\varepsilon_D(\lambda_D)}\left(\frac{F_{DA}(\lambda_A)}{F_A(\lambda_A)} - 1\right) \tag{3b}$$

where λ_D and λ_A denote the donor and acceptor excitation wavelength, $\varepsilon_D(\lambda)$ is the donor absorbance at wavelength λ (and likewise for the acceptor), and $F_D(\lambda)$ is the donor fluorescence at wavelength λ. We finally used the decrease in donor lifetime in the presence of acceptor,

$$E^{(c)} = 1 - \tau_{DA}/\tau_D \tag{3c}$$

as a readout for estimating the FRET efficiency.

Finally, assuming a Förster-type (dipole−dipole) interaction between donor and acceptor, and N as the number of acceptors per donor

$$E(N, r) = N/\left(N + (r/R_0)^6\right) \tag{3d}$$

Estimate of the Donor−Acceptor Ratio. Absorption spectra were obtained on a UV−vis spectrometer (Agilent Technologies). ATTO absorption at 450 nm is negligible to that of the NCs. Conversely, all NC samples hardly absorb at the ATTO absorption peak (597 nm). Thus, measuring the absorbance at 450 and 597 nm, respectively, allowed the determination of [NC] and [ATTO]. All spectra were corrected for background with a blank run.

Fluorescence emission spectra were recorded upon 450 nm (donor excitation) or 590 nm (direct acceptor excitation) on a Fluorolog-3 spectrofluorometer (HORIBA Jobin Yvon, Japan) and were corrected for the instrument response.

After gel electrophoresis, we estimated the number of ATTO dyes per NC donor in the purified samples by the six following steps (Figure 2).

1. The three reference absorption spectra were measured: sample (1), NC−polymer; sample (2), NC−polymer−ATTO 1%; and sample (3), ATTO−polymer 1% in the absence of NC (EP).
2. From Lambert−Beer's law ($A = -\log_{10}(I/I_0) = \varepsilon cL$), using $\varepsilon_{597} = 120\,000\ M^{-1}\,cm^{-1}$ of ATTO dye at absorption maximum, the concentration of ATTO in sample (2) was estimated as 1.03 μM.
3. The spectrum of sample (3) was scaled up to match the measured absorption maximum of sample (2) at the ATTO absorption maximum. This scaled spectrum is referred to as sample (3)′ in the following. For the example shown in Figure 2, the scaling factor was 0.9789 (0.12082/0.12342), from the measured absorption of samples (2) and (3) at 597 nm (Figure 2B).

(26) Striolo, A.; Ward, J.; Prausnitz, J. M.; Parak, W. J.; Zanchet, D.; Gerion, D.; Milliron, D. J.; Alivisatos, A. P. *J. Phys. Chem. B* **2002**, *106*(21), 5500–5505.

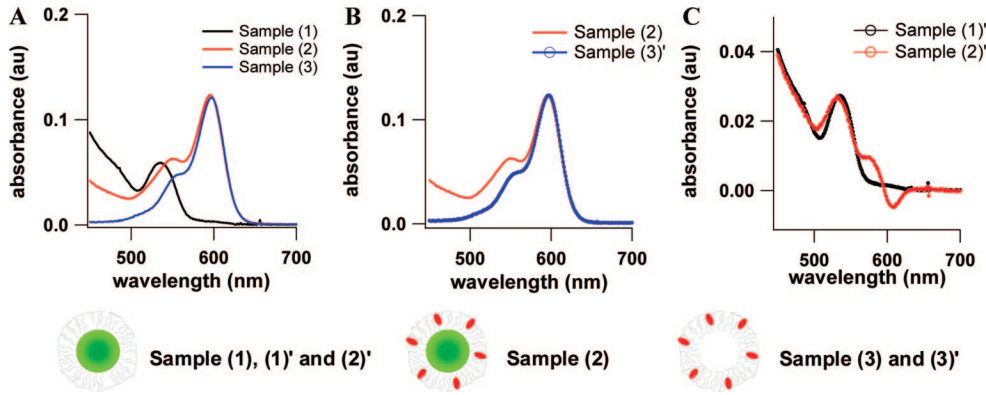

Figure 2. Estimation of the number of ATTO/NC. (A) Samples (1), (2), and (3) indicate absorbance spectra of purified, polymer-coated Evident NC, 1% ATTO−polymer-coated Evident NC, and 1% ATTO−polymer micelles (EP), respectively. (B) and (C) describe the scaling procedure. See text for details.

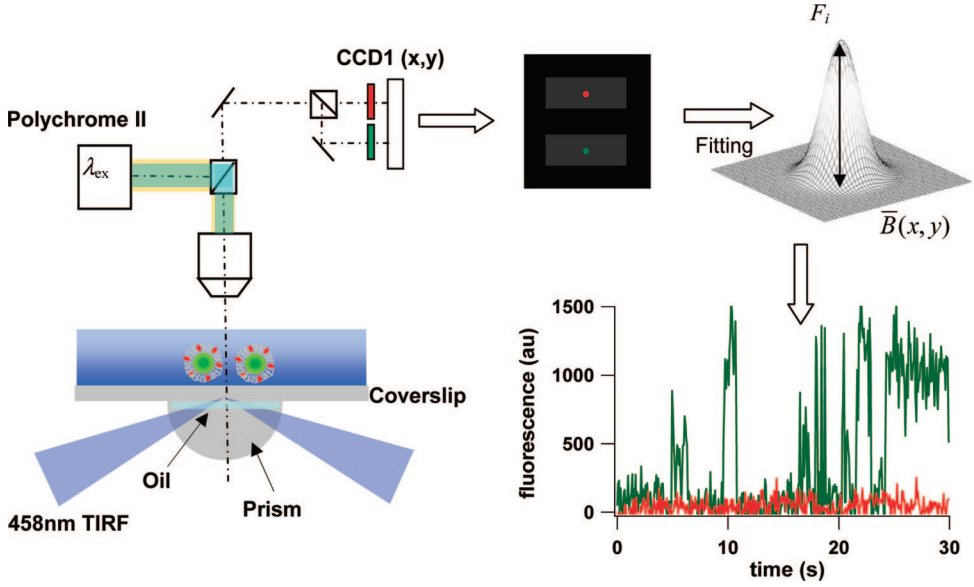

Figure 3. Schematic representation of the setup used for spFRET detection and subsequent data analysis. spFRET was detected on an upright fluorescence microscope fitted for combined epifluorescence and total internal reflection fluorescence (TIRF). We used the "prism-type" configuration, with an external prism and coverslip made of Schott SUPRASIL 311 coupled through a thin layer of ultralow autofluorescence immersion oil. Fluorescence was detected through a water immersion objective and directed, after the splitting of donor (green) and acceptor (red) fluorescence and appropriate filtering, on an electron-multiplying charge-coupled device (CCD) detector. Dual-color images containing a single FRET pair were excised and submitted to a PSF-fitting routine for the measurement of background $\bar{B}(x,y)$and spot *Fi* fluorescence (see Materials and Methods). Traces at the bottom right show blinking fluorescence of a naked NC and the corresponding trace in the red channel.

4. Next, we subtracted the spectrum of sample (3)′ from that of sample (2), thus obtaining a difference spectrum (called (2)′) indicative of the absorption of the NC alone, after subtraction of the ATTO component (Figure 2C). The obtained spectrum compares favorably with a scaled version of spectrum (1), termed sample (1)′ in Figure 2C.
5. From (2)′, the first exciton peak of polymer-coated NCs is measured at 532 nm with an amplitude 0.02731, so that we can calculate the concentration of polymer-coated NCs in sample (2) as 0.33 μM, again using Beer−Lambert's law and assuming $\varepsilon_{max} \sim 82\,000\ M^{-1}\ cm^{-1}$ at the first exciton peak.
6. Finally, the number of ATTO per NC is obtained by dividing the concentrations of ATTO and NCs, 1.03/0.33 = 3.1.

Single-Particle FRET (spFRET) Detection. For spFRET and TSCSPC (time- and space-correlated single-photon counting) measurements, glass coverslips (25 × 10 mm, Menzel, Braunschweig, Germany) were prepared for imaging by successive sonication in absolute ethanol, acetone, HNO_3, and 6 N KOH solutions for 20 min and subsequently washed three times with Milli-Q water. To remove unwanted autofluorescence, they were cured with UV light emitted from a HBO50 lamp during 30 min.

NCs were diluted 100 times from a ~0.2 μM stock in 50 mM borate buffer at pH 9.0. Droplets of 10 μL were dispersed on coverslips and allowed to dry. The coverslips were subsequently washed three times to remove free dye, micelles, and nonattached complexes. NCs remained stably attached to the glass surface in aqueous solution during several hours. For TSCSPC experiments, these coverslips were mounted on microscope slides (76 × 26 × 1 mm LLR2, CML, Nemours, France) and sealed with colorless nail varnish. All samples were stored in the dark at +4 °C until observation.

spFRET measurements were carried out on a custom upright microscope equipped for combined epifluorescence and prism-type evanescent-field excitation (Figure 3, left). Polychrome II (TILL Photonics, Gräfelfing, Germany) provided narrowband (18 nm fwhm intensity) polychromatic epifluorescence excitation which was used for localizing and focusing at the glass surface and for the recording of fluorescence excitation spectra.

For evanescent-field excitation, the beam of a multiline Ar^+-ion laser (<5mW at 458 nm impinging on the sample, Reliant 150, Laser Physics, Milton Green, Cheshire, U.K.) was directed at an oblique angle at a ultralow autofluorescence hemicylindrical prism (Suprasil-311, Bernhard Halle Nachfahren, Berlin, Germany).

Penetration depth depended on the angle of incidence of the laser beam and was of the order of 150 nm throughout.

Fluorescence was detected through a LUMFL 60×/1.1-NA water immersion lens (Olympus, Hamburg, Germany) and spectrally separated into a donor and acceptor fluorescence channel (W-view, Hamamatsu, Hamamatsu City, Japan), and directed on a QuantEM 512SC electron-multiplying charge-coupled device (CCD) camera (16 μm × 16 μm pixel size, Photometrics, Tucson, AZ). Images were acquired and analyzed with MetaMorph (Molecular Devices, Sunnyvale, CA). Acquisition rates were 5 or 10 Hz, with exposure times of 75−100 ms for imaging.

For point-spread function fitting and FRET quantification, we first averaged 400−500 image frames of a time-lapse movie and identified regions of interest (ROIs) containing a single NC donor. Individual NCs were recognized by their intensity and blinking; see, for example, Figure 3.

To improve the signal-to-noise ratio, we used a point-spread function (PSF) fitting approach. We used this approach (i) to localize corresponding objects in the donor and acceptor channel and correct for subpixel shift between the color channels, and (ii) to measure the background, amplitude, and width for of spots in the donor and acceptor channel. Image subregions (7 × 7 pixel) were excised from the dual-color fluorescence images and fitted with a two-dimensional (2-D) Gaussian (IGOR, Wavemetrics, Lake Oswego, OR),

$$F(x_i, y_i) = \bar{B}(x, y) + F_i \exp\left[-\frac{1}{2}\left(\left(\frac{x - x_i}{\delta_x}\right)^2 + \left(\frac{y - y_i}{\delta_y}\right)^2\right)\right] \quad (4)$$

where (x_i, y_i) and δx and δy are the center position and widths of the 2-D Gaussian and $\bar{B}(x,y)$ is the average background in the ROI of interest. For each batch, we report F_i for 20−30 ROIs per coverslip and average over at least three different coverslips.

On 458 nm evanescent-wave excited dual-color fluorescence images of single NCs, we proceeded analogously. We first extracted from the acceptor image ROIs containing a single fluorescent spot and transferred these ROIs onto the donor image. Pairs were retained if they represented detectable acceptor fluorescence as well as donor blinking, indicating a single NC donor at the origin of the detected acceptor fluorescence. Thus, our choice is biased toward bright FRET pairs with negligible donor quenching and moderate duty cycles.

Time- and Space-Correlated Single-Photon Counting (TSCSPC) Measurements. Shortening of the donor fluorescence lifetime in the presence of the acceptor or ingrowth of acceptor lifetime has been used here to quantify FRET efficiencies.[6,12] Lifetime measurements provide an intensity-independent readout of FRET efficiency, which is important when dealing with dim objects as in the present case. Here, we used TSCSPC to reveal the heterogeneity of donor photoluminescence decays within a given batch of NCs. Donor decays were recorded on a Leica SP2 inverted microscope equipped with a Leica TCSP2 confocal scan head (Leica, Solms, Germany). Donor photoluminescence was excited at 802 nm with a femtosecond-pulsed Ti:sapphire laser (100−200 fs, 80 MHz, MaiTai, Spectra Physics, Newport, CA), collected through a HQ 560/40m emission band-pass (Chroma Technology) to reject acceptor fluorescence, and detected on a microchannel plate (MCP) imaging detector (Hamamatsu R3809U-50, Japan). A TCSPC board (SPC-730, Becker & Hickl, Berlin, Germany) was used for the acquisition of both excitation light pulse and fluorescence emission. Typical durations to accumulate enough photons were 2000 s. The time scaling was 37.4 ps/channel, and 4096 channels were used. The instrument response following the laser pulse (100 ps, fwhm) was recorded by detecting the light scattered by a water solution. The large 2PEF cross sections of NC donors permitted the use of low average power (~1 μW). With a 2PEF cross section of ~7000 GM for 525−CdSe−ZnS NCs and ~100 GM for ATTO594, we expect the donor to be the predominantly excited species.[27]

The MCP detector allowed spatially resolved decay measurements (1.5 μm/pixel in the object plane). Binning increased the signal-to-noise ratio, at the expense of spatial resolution. In the later case, the measured decay is the ensemble average of all the NCs present in the binned megapixel. Analysis of the fluorescence decay used either the maximum entropy method[28] or a sum-of-exponentials method implemented in the Becker & Hickl SPCImage software. With the maximal entropy method, we obtained three lifetimes for all samples. Two shorter lifetimes were in the range of 0.2−0.3 ns and 0.8−0.9 ns, and a third longer lifetime component was of the order of 13−21 ns. The sum-of-exponentials method which only gave access to the two shorter lifetimes because of its 10 ns time window is more restrictive, since both χ^2 and the number of exponentials are fixed. We systematically rejected fits with $\chi^2 > 1.2$. The latter approach therefore yields lifetime values similar to those obtained in cuvette measurements, but with the additional information of the spatial distribution. Therefore, histograms of τ values could be obtained by sampling donor lifetimes at different regions of the coverslip.

Results and Discussion

For the synthesis of our NC−ATTO FRET system, an amphiphilic polymer was built by linking a hydrophobic side chain to a backbone of poly(isobutylene-alt-maleic anhydride), as previously described.[6,24] We chose the conditions so that 75% of the anhydride monomers reacted with one dodecyl hydrophobic chain, leaving the remaining 25% vacant for other couplings

As an acceptor fluorophore, we incorporated ATTO590-NH_2 dye (ex/em = 594/624 nm, extinction $\varepsilon_{594} = 120\,000\ M^{-1}\ cm^{-1}$, quantum yield $\phi = 0.8$, fluorescence lifetime $\tau = 3.7$ ns; see Figure 1 for details) by amide linkage to the vacant anhydride monomer positions. By systematically changing the stoichiometric ratio during synthesis, a series of amphiphilic polymers with increasing concentrations of ATTO dye from 0.01% up to 4% (referring to the percentage of anhydride rings in the polymer which are linked to ATTO dye molecules) were preassembled and, upon opening in aqueous medium of the still vacant anhydride which frees negatively charged carboxyl groups, used to colloidally stabilize NCs. We used as donors either EviDots 560 (Evident Technologies), QDot 565 ITK (organic quantum dots, Invitrogen), or homemade CdSe/ZnS and CdSe only nanocrystals.[29,30]

After core−shell assembly, colloidal NCs were purified by gel electrophoresis as described earlier,[31] thereby separating empty polymer micelles (EP) from coated and dye-loaded NCs [6]

Thus, controlling sensor assembly, we investigated how the FRET efficiency varied with the acceptor/donor ratio. Samples synthesized with acceptor varying from 0.01% to 4% were prepared from a *same* batch of NC donors, working either at the same concentration of ATTO dye (Figure 4A, B) or at the same concentration of NCs (Figure 4C, D), adjusting their concentrations so as to obtain identical absorbance at either 597 or 450 nm, respectively (see Materials and Methods). Donor excitation at 450 nm resulted in detectable fluorescence from both Evident NCs and ATTO590, despite the only negligible direct excitation of the acceptor (Figure 4A, C), thus indicating the transfer of excitation from the NC donor to the ATTO acceptor. As expected from a multiple-acceptor system, the yellow-green peak NC

(27) Clapp, A. R.; Pons, T.; Medintz, I. L.; Delehanty, J. B.; Melinger, J. S.; Tiefenbrunn, T.; Dawson, P. E.; Fisher, B. R.; O'Rourke, B.; Mattoussi, H. *Adv. Mater.* **2007**, *19*, 1921–1926.

(28) Brochon, J. C. *Numerical computer methods*, Part B; Academic Press: San Diego, CA, 1994; Vol. *240*, pp 262−311.

(29) Dabbousi, B. O.; Rodriguez-Viejo, J.; Mikulec, F. V.; Heine, J. R.; Mattoussi, H.; Ober, R.; Jensen, K. F.; Bawendi, M. G. *J. Phys. Chem. B* **1997**, *101*(46), 9463–9475.

(30) Reiss, P.; Bleuse, J.; Pron, A. *Nano Lett.* **2002**, *2*(7), 781–784.

(31) Parak, W. J.; Gerion, D.; Zanchet, D.; Woerz, A. S.; Pellegrino, T.; Micheel, C.; Williams, S. C.; Seitz, M.; Bruehl, R. E.; Bryant, Z.; Bustamante, C.; Bertozzi, C. R.; Alivisatos, A. P. *Chem. Mater.* **2002**, *14*(5), 2113–2119.

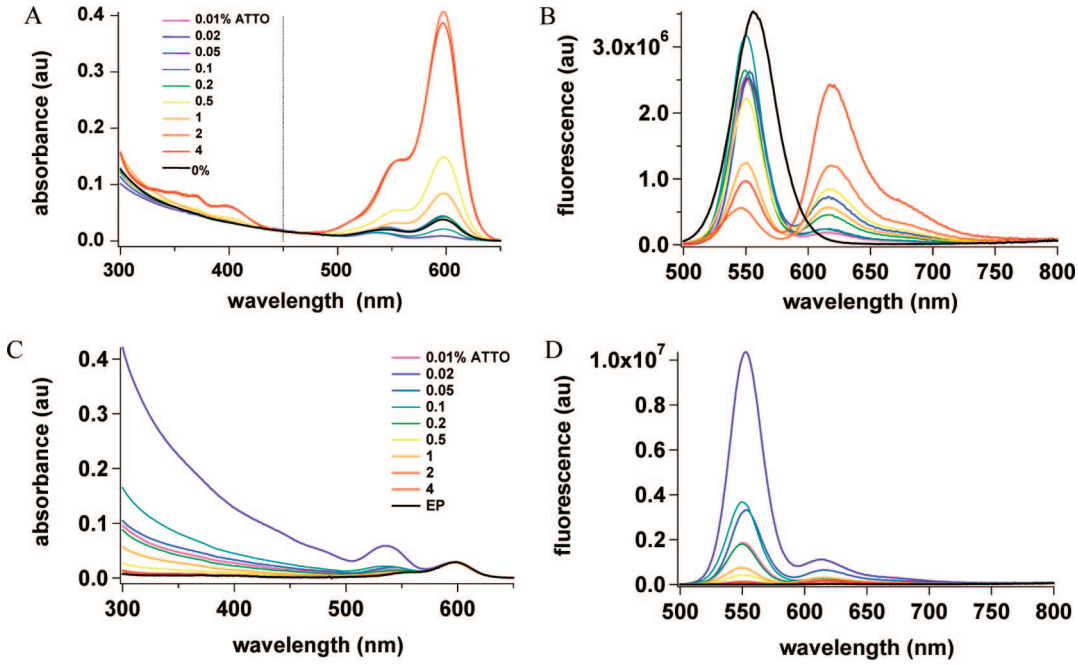

Figure 4. Dependence of normalized absorbance (left) and fluorescence emission (right) on acceptor concentration. A single batch of Evident nanocrystal (NC) donors was coated with ATTO−polymers with an ATTO load increasing from 0.01% to 4%. The percentage refers to the ratio of ATTO molecules to the number of anhydride rings making up the polymer backbone. EPs are empty polymer micelles (2% ATTO) extracted by gel electrophoresis,[6] and Evident NC (0% ATTO) denotes the polymer-coated bare donor, in the absence of acceptor fluorophores. For fluorescence spectra, conditions where adjusted by dilution/concentration of the samples so as to have the same concentration of NCs (absorbance measured at 450 nm, panel (A)) or of ATTO dye (absorbance measurement at 597 nm, panel (C)). (B) and (D) show the corresponding fluorescence emission spectra of the same samples as in (A) and (C) upon donor excitation at 450 nm. Note the increasing transfer of energy from the donor (emission peaking at 560 nm) to the acceptor, ATTO 590 (with 622 nm peak emission) upon increasing the concentration of the later.

emission systematically decreased with increasing ATTO concentration, illustrating the dose-dependent quenching of donor PL emission.[32] We observed a concomitant increase in the ATTO dye emission, indicating the energy absorbed by the donor sensitized acceptor fluorescence in a concentration-dependent manner. Notably, for an equal amount of donor, the total energy that was radiatively emitted as donor PL and acceptor fluorescence (i.e., the area of the spectrum) stayed roughly constant over the entire range of ATTO concentration, indicating that the addition of ATTO does not increase the fraction of dark reactions relaxing NC excitation states compared to bare NCs.

We next experimentally determined the actual acceptor/donor ratio, by successively comparing the absorbance of pairs of polymer−ATTO/NC−polymer−ATTO and NC−polymer/NC−polymer−ATTO. The concentration of ATTO in polymer was directly read off from its absorbance at 594 nm. Since ATTO was preloaded to the polymer before NC coating and NCs only negligibly absorb at 594 nm,[6] the absorbances of ATTO in polymer and in coated NCs could be scaled (see Materials and Methods). Subtracting the two latter spectra generates an artificial compound NC−polymer spectrum that closely reproduces the measured NC−polymer spectrum, with the exception of two small antiphasic deviations suggesting a slight peak shift of the donor or acceptor when conjugated (see Figure 2 in Materials and Methods). Conversely, the amount of NCs included in the NC−polymer−ATTO complexes was directly estimated from absorbance measurements at 450 nm where ATTO absorbance is negligible compared to that of the NCs. The acceptor/donor ratio is then given by the ratio of the measured amounts of ATTO and NCs. From these measurements, we estimate that varying between 0% and 4% the number of monomers building up the polymer resulted in embedding 0−20 molecules of ATTO dye per NC. For example, NCs prepared with "1%" ATTO−polymer contained, on average, five ATTO dye acceptors (see Figure 5A).

Using this stoichiometry calibration, we next quantified these notions by graphing evolution with A/D of the NC peak emission at 565 nm, as well as the sensitized donor fluorescence at 627 nm peak according to eq 3a (Figure 5B, left). From these data, we calculated the FRET efficiency E using either donor quenching or sensitized acceptor fluorescence as a parameter (Figure 5B, right). As expected for multiacceptor FRET, we observe an initial dependence of E on the number of acceptors and a plateau of ~0.65 for >5 acceptors.

How does this observation compare with theory? If we fit eq 3d, $E(N,r) = N/(N+(r/R_0)^p)$ with the experimental data while keeping $p = 6$ fixed, we find $r/R_0 = 1.11 \pm 0.04$, close to 0.77−1.08 predicted from ref 33. Two independent experiments confirmed these bulk cuvette measurements. First, single-pair FRET (spFRET) data obtained from individual NCs images on total-internal reflection fluorescence images (open squares in Figure 5B right) showed the same dependence of donor PL on the A/D ratio ($r/R_0 = 1.09 \pm 0.23$), indicating that our population average was not biased through the existence of bright subpopulations, NC aggregation, or low spectrometer sensitivity. Conversely, the presence of a dielectric interface in evanescent-wave excited fluorescence does only marginally, if at all, affect FRET. Letting both p and r/R_0 run freely in fits of $E(N,r)$ gave 5.6145 ± 1.9 and 1.09 ± 0.34 as best fit parameters. Nevertheless, the dispersion of the data would have allowed other suitable combinations of p and r/R_0 with $p \in (2, 6.5)$ to produce a similar precision (see gray trace in Figure 5B right)

(32) Schmelz, O.; Mews, A.; Basché, T.; Herrmann, A.; Müllen, K. *Langmuir* **2001**, *17*, 2861–2865.

(33) Sperling, R. A.; Liedl, T.; Duhr, S.; Kudera, S.; Zanella, M.; Lin, C.-A. J.; Chang, W. H.; Braun, D.; Parak, W. J. *J. Phys. Chem. C* **2007**, *111*, 11552–11559.

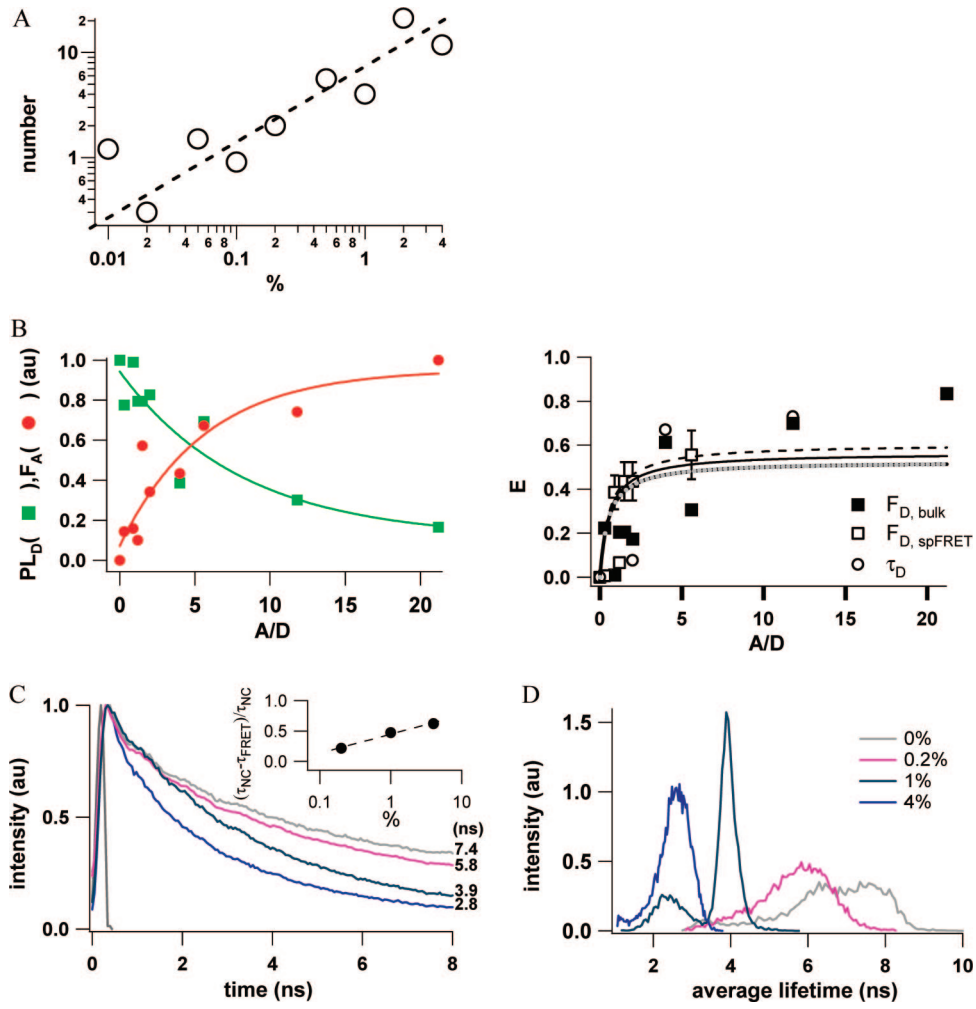

Figure 5. FRET efficiency of the Evident NC/ATTO system as a function of the polymer/ATTO stoichiometry and the number of ATTO molecules actually bound per NC. (A) Log−log plot of the measured relationship between percentages of ATTO included during polymer synthesis and ATTO molecules actually decorating the central NC donor. Points show mean values for three batches. Slope is 4−5. (B) Left: evolution with acceptor/donor ratio (A/D) of donor photoluminescence (PL_D, green rectangles) and sensitized donor fluorescence (F_A, red dots), measured as the peak of spectral donor and acceptor emission at 565 and 627 nm, respectively. Solid lines are to guide the eye. Right: transfer efficiency E as a function of A/D, measured from bulk cuvette photospectrometry, single-donor PL on TIRF images, or average donor lifetime obtained from time- and space-correlated single-photon counting (TSCSPC) measurements. (C) Examples of time-dependent fluorescence recordings for EviDot560 donors with different number of ATTO dye as indicated. Numbers denote average lifetimes calculated according to the maximum-entropy method. Pixel bin was 2 × 2, and total integration time was 2000s. (D) Average lifetime histograms for the different Evident NC samples shown in panel (B). Histograms are normalized to equal area. Note the broad and skewed lifetime distributions, even for bare NCs without ATTO dye.

Second, two-photon excitation time- and space-correlated single-photon counting (TSCSPC) showed a pronounced decrease in donor lifetimes for NC/ATTO assemblies compared with unconjugated NCs (Figure 5C). As expected, excited-state lifetimes dropped with increasing number of ATTO acceptors. Mean average decay times $\langle\tau\rangle$ for bare polymer-coated NCs were around 7 ns, whereas the maximal embedding of 20 dye molecules ("4%") reduced this value to 2.5 ns. Thus, time-resolved fluorescence independently corroborates our bulk and spFRET intensity data that FRET provides an efficient alternative route for donor relaxation, yielding, for $p = 6$ and high N, a limiting $E_{fit}^{\infty} = 1 - \tau_{DA}/\tau_D = 0.55$, very similar to the 0.51 from bulk and 0.59 TIRF measurements.

Fluorescence lifetime imaging microscopy (FLIM) analysis also allowed us to obtain spatially resolved donor fluorescence decays from FRET nanoprobes immobilized at a low density on a glass coverslip. Figure 5C quantifies the effect of increasing acceptor concentration in terms of distributions of single-pixel donor lifetimes. Even without acceptor, the distribution is relatively large and skewed to the short end. Although the effective pixel size (1.5 × 1.5 μm in the object plane) of our microchannel plate detector prohibited the detection of spFRET from individual nanoprobes (1 pixel containing some 1−5 NCs), the spatial sampling was fine enough to reveal an important heterogeneity of donor lifetimes within a given batch of NC donor and ATTO concentration. The spread of $\langle\tau\rangle$ was not due to pixel noise, because pixel binning resulted in average values reproducing the distribution means of single data (Figure 5C right). Thus, FLIM suggests that donor PL is influenced by factors other than FRET alone and probably linked to sample aging, aggregation, or photodegradation.

In the present work, we stoichiometrically embedded hydrophobic dye molecules in amphiphilic polymer micelles. Using these preassembled micelles to wrap NCs shells, we control the mean number of ATTO acceptor molecules bound per NC donor from 0 to 20. In this range, the intrinsic properties of the NC−ATTO dye complex as measured by the intensity and lifetime of the donor decreased monotonously with ATTO concentration. Our results provide the direct experimental demonstration that,

at a fixed A/D distance, multiacceptor FRET provides an efficient means to increasing the sensitivity of FRET-based nanoprobes.

Polymer wrapping is a rigid process, thereby fixing the donor/acceptor distance. However, a narrow distribution of the distances within the polymer shell critically depends on the tight wrapping of the NC central donor with the polymer coat. In this context, it is important to note that our experimental data are the size measurements derived from the hydrodynamic radii.[33] However, we can be sure that the inclusion of ATTO (at any percentage) does not change the geometry of the polymer shell, as the hydrodynamic radii are independent of the ATTO percentage. Also, donor/acceptor distance should fall within the smaller and bigger limits defined by the middle of the polymer shell and the outside of the polymer shell, respectively. However, we cannot exclude that the polymer shell detaches with time, resulting in a potentially larger distribution.

Irrespective of the precise distribution of donor/acceptor distances, our result of a monotonic dependence of the FRET efficiency on the acceptor concentration is different from the bell-shaped dependence of the FRET efficiency on the A/D ratio observed for a CdTe/Rhodamine B system,[5] where the drop in transfer efficiency at acceptor excess may reflect acceptor/acceptor or donor/donor interactions in the densely packed film used, similar to what has been suggested for crowded environments, where significant excitation transfer can occur via states that are optically dark.[34]

Emission-based FRET detection works best within a limited range of molar acceptor/donor ratios.[35] Although FLIM-FRET[36] is less restricted in this respect, the measurement of E and the estimation of interacting versus noninteracting species are simplified when the donor and acceptor are present at fixed molar ratios. Stoichiometric inclusion by preloading polymers permits one to tailor FRET pairs through a chemical variable that can be controlled during synthesis and nanoprobe assembly. It therefore adds a degree of freedom to nanosensor assembly beyond the existing choice of spectrally suitable donors and acceptors and tuning their separation distances through the use of molecular linkers. The capacity to fine tune the transfer efficiency will be of particular importance for sensors that derive their contrast from changes in donor/acceptor spectral overlap, where an E value close to 0.5 would maximize sensitivity, or for ratiometric constant-distance polymer-shell sensors for which one might want to find conditions that go along with incomplete donor quenching yet detectable acceptor fluorescence.

The observed heterogeneity among nominally identical NC donors complicates calibrated analyte sensing and implies that checkpoints need to be introduced at critical points of synthesis and sensor assembly. Alternatively, microfluidic postsynthesis recognition and sorting might provide more homogeneous sensor performance.[37] Thus, although FRET-based hybrid NC/fluorophore assemblies hold important promises for being the next generation of nanobiosensors, to work in nanoscale biological environments, the technique still needs further development.

Acknowledgment. This work was supported by the *Groupement d'intérêt Publique - Agence Nationale de la Recherche Programme Nanosciences et Nanotechnologies* (GIP-ANR PNANO, Grant No. ANR-05-NANO-051 "NanoFRET" to J.-M.M., A.F., M.O., and W.J.P.) and, in parts, by the European Union (Grant Nos. FP6-2004-013880 "Single-motor FLIN", FP6-2005-019481 "From FLIM to FLIN", and FP6-2006-037897 "AUTOSCREEN" to M.O.) and the German Research Foundation DFG (W.J.P., SPP 1313 PA 794/4-1). A.V.Y., C.L., and S.G. were postdoctoral fellows funded by the *Centre National de la Recherche* (CNRS), the *Fondation pour la Recherche Médicale* (FRM), and GIP-ANR, respectively. The authors thank Ralph Sperling and Marco Zanella for discussion.

Supporting Information Available: Synthesis of the polymer and preparation of homemade nanocrystals, estimation of photoluminescence quantum yields of NC donors, electrophoretic purification of NC−ATTO complexes, ensemble FRET measurements in cuvette, FRET efficiency as a function of donor/acceptor ratio, and single-particle FRET (spFRET) data and TSCSPC FLIM data for Invitrogen NCs (Qdot565) and homemade CdSe/ZnS as well as CdSe NCs. This material is available free of charge via the Internet at http://pubs.acs.org.

LA8038347

(34) Zimet, D. B.; Thevenin, B. J.-M.; Verkman, A. S.; Shohet, S. B.; Abney, J. R. *Biophys. J.* **1995**, *68*, 1592–1603.
(35) Barney, C.; Danuser, G. *Biophys. J.* **2003**, *84*, 3992–4010.
(36) Becker, W.; Bergmann, A.; Hink, M. A.; König, K.; Benndorf, K.; Biskup, C. *Microsc. Res. Tech.* **2004**, *63*, 58–66.
(37) Chang, J.-Y.; Yang, C.-H.; Huang, K.-S. *Nanotechnology* **2007**, *18*, 305305.